Preprints of the 2012 20th Mediterranean Conference on Control & Automation (MED), Barcelona, Spain, July 3-6, 2012

Power-Oriented Graph in automotive application: VVT modeling on Lamborghini V12 engine

Christian Corvino
Automobili Lamborghini SpA
Research and Development Dept.
Via Modena 12, 40019, Sant'Agata Bolognese (BO), Italy
Telephone: +39 051 959 7967
Email: cristian@corvino.lamborghini.com

Roberto Zanasi
University of Modena and Reggio Emilia
Via Vignolese 905, 41100, Modena, Italy
Telephone: +39 059 2056 161
Fax: +39 059 2056 126
Email: roberto.zanasi@unimore.it

***Abstract*—In automotive applications the emission reduction and fuel consumption are relevant goals for manufactures so that several devices are introduce in the engine. One of such devices is Variable Valve Timing (VVT), modeled in this paper, that represents a complex multi physic system designed to control the intake camshaft: by opening and closing time of inlet and outlet valves are modified so that the engine conditions can satisfy the gaols in term of torque improvement in all the speed ranges as well as increasing fuel economy and reducing exhaust emission. In this paper the Power Oriented Graph (POG) technique has been used for modeling the considered electromechanical system allowing to detect some hide variables not readable by the sensors. The effectiveness of the proposed model has been validated using an experimental set-ut.**

INTRODUCTION

The VVT device offers benefits in fuel economy, performance and emission levels of the gasoline engines ([Leone et al., 1999], [Gray, 1988], [Ma, 1988], [Stein and Galietti, 1995]). Most of the advantages in emission reduction, both NOx and HC, is related to the internal EGR (Exhaust Gas Recirculation) mechanism realizable by VVT. This mechanism reduces the pumping losses and improves the fuel economy by cam timing optimization over a wide range of engine operations conditions. Good idle quality (minimum overlap) and improved wide open throttle provide high speed performance (maximum inducted air change). The old cam phasers were built with helical splines that could be shifted axially with the engine oil pressure via 4-way oil control valve (OCV). Friction associated with the splines connections limits the transmission of cam torque disturbance into the oil system so that the pressure fluctuations are dampened. The newer vane type cam phasers are more compact, faster and operate even at low oil pressure, eliminating the energy loss due to the spline mechanism, but they show a greater cam torque disturbance, pressure and position oscillations. Vane phasers include usually a locking pin that transmits the cam torque at the engine starts, when the oil pressure is not enough for actuating it. Once the engine has reached the minimum oil pressure, the locking pin retracts and it is non longer active. The vane type cam phaser and the 4-way oil control valve (OCV) along with the engine oil system is a simple and economic way for cam shifting implementation ([Gauthier et al., 2005]).

The paper is organized as follows. A brief introduction of the Power-Oriented Graph technique is given in Sec. I. A detailed description of the considered electromechanical system is reported in Sec. II. The POG dynamic model of the VVT system is given in Sec. III, while in Sec. IV the proposed model is validated using an experimental set-up. The paper ends with some conclusions in Sec. V.

I. THE POWER-ORIENTED GRAPHS PRINCIPLES

The Power-Oriented Graphs are block diagrams combined with a particular modular structure essentially based on the two blocks shown in Fig. 1: the *elaboration block* $(e.b.)$ which stores and/or dissipates energy (i.e. springs, masses, dampers, capacities, inductances, resistance, etc.) and the *connection block* $(c.b.)$ which redistributes the power within the system without storing nor dissipating energy (i.e. transformers, gear reduction, etc.). Both of blocks are suitable for representing scalar and vectorial system: matrix $\mathbf{G}(s)$ is always a square matrix composed by positive real transfer functions, matrix $\mathbf{K}$ can also be rectangular. The black spot present in the $e.b.$ stands for a minus sign that multiplies the entering variable. The main feature of the POG block schemes is the direct correspondence between pairs of variables and real power flows: the scalar product $\mathbf{x}^{\mathrm{T}}\mathbf{y}$ of the two vectors involved in each dashed line of the POG block scheme, see Fig. 1, has always the physical meaning of "*power flowing through that particular section*".

II. THE PHYSICAL SYSTEM

In a four stroke Internal Combustion Engine (ICE) the phase of the engine cycle, during which the inlet and exhaust valves are open, is usually referred to "*valve timing*" and is measured as the opening and closing angles,

978-1-4673-2529-5/12/$31.00 ©2012 IEEE

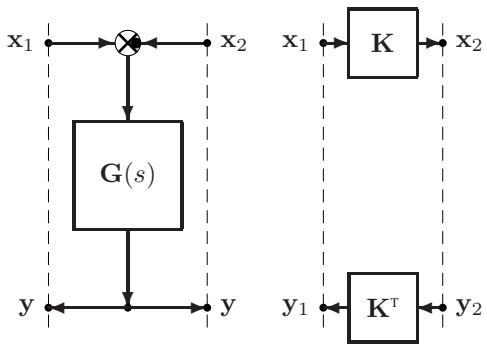

(a) Elaboration block. (b) Connection block.

Fig. 1. Power Oriented Graph basic blocks.

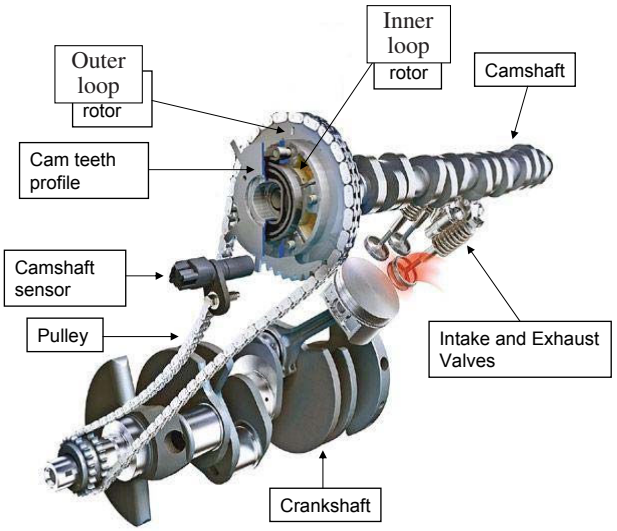

Fig. 2. VVT system overview.

for both inlet and exhaust valves, before or after the point at which the piston reaches the top death center (TDC) or the bottom death center (BDC). In conventional engines the valve phasing time and their lift are fixed, so they don't vary over the entire engine speed and load range. In this case the valve phasing time is chosen after adequate evaluations on fuel consumption, pollution emission, engine torque and idle stability. Due to the dynamics of the gas flows into the cylinder and through the valves, the engine breathing changes during the normal engine operation, so the fixed valve timing can satisfy a particular engine speed and load situation at the cost of poorer performances over the rest of the range. In order to reach a better performance at high speed with a flatter torque and in order to operate efficiently at wider range of speed, the ICE are often equipped with variable valve timing and/or lift ([Stone et al., 1988]). For example, a van may adopt less overlapping for the benefits of low speed output, while a racing engine may adopt considerable overlapping for high speed power. On the other hand, an ordinary sedan may adopt valve timing optimized for mid-rev so that both the low speed drivability and high speed output will not be sacrificed too much. No matter which one, the result is just optimized for a particular speed. With Variable Valve Timing ([Buchinger et al., 1998]), power and torque can be optimized across a wide engine revs such that:

1) the engine can rev higher, thus raises peak power;
2) at low-speed the torque increases improving the drivability.

As noticed, the main purpose of the system is to shift rapidly the actual cam position toward the desired value implementing a closed loop control to meet a certain response time useful for emission and drivability. The system showed in Fig. 2 is composed by an *inner rotor* directly linked to the camshaft by screw thread and an *outer rotor* directly connected to the crankshaft by pulley: J_r and J_s will denote the inertias of the two rotors. During the normal engine operation the outer rotor runs at an half of the engine speed revolution, while the inner rotor is pushed against the outer rotor face due to contemporary work of the spring return, used for replacing as fast as possible when the valve timing is not required, and the oil pressure delivered by the OCV when not actuated. Furthermore the pin blocks the outer rotor angle displacement if no enough pressure is reached. In this situation the VVT is off and no relative angle movement between inner and outer rotors is possible. Once the engine has reached a minimum oil pressure, the pin retracts, so it is no longer active, and the outer rotor can start moving. From now on, the generated shifting angle, defined as the difference between the stator and rotor angles respect to the TDC, is controlled by the engine control unit. When VVT is on, a proper control strategy of the OCV system allows to the oil pressure to reach one of the two cam vanes present between the inner and outer rotors: in one of the two cam vanes the oil pressure increases, while the other is unfilled becose directly connected to the return oil tank.

III. The POG model of the VVT system

The VVT system presents two degrees of freedom: the outer rotor position ϑ_s and the inner rotor position ϑ_r. The POG block scheme describing the dynamics of the VVT system is shown in Fig. 4. The main mechanical and hydraulic parameters used for modeling the VVT system are shown in Tab. I. The VVT system can be described as the cascade of four interacting subsystems (see Fig. 4): 1) the OCV valve, 2) the pin dynamics, 3) the hydraulic dynamics of the vane chambers and 4) the inner rotor. Each subsystem is graphically described by a particular section of the POG block scheme shown in Fig. 4.

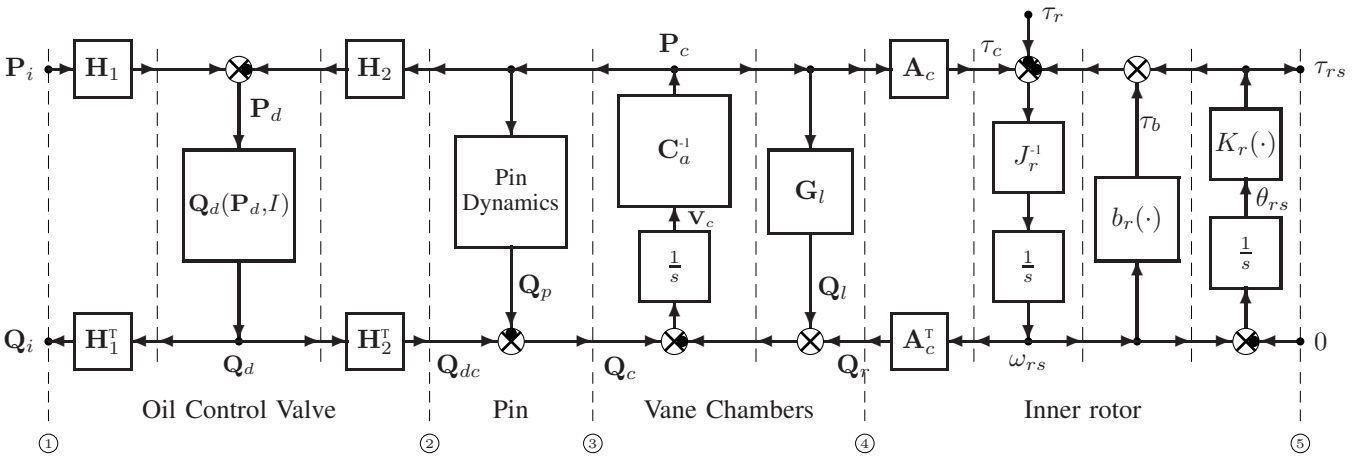

Fig. 4. POG block scheme describing the dynamic model of the VVT system.

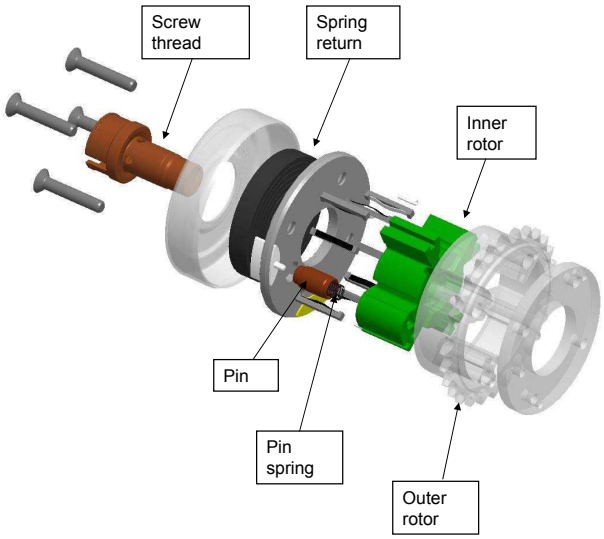

Fig. 3. The essential mechanical elements of the VVT system.

P, R	input and return oil pressures
Q_p, Q_r	input and return oil volume flow rates
Q_{p1}, Q_{p2}	oil volume flow rates from power supply to vane chambers
Q_{r1}, Q_{r2}	oil volume flow rates from return to vane chambers
C_{p1}, C_{p2}	flow rates coefficients from power supply to vane chambers
C_{r1}, C_{r2}	flow rates coefficients from return to vane chambers
P_{c1}, P_{c2}	oil pressures in the vane chambers
Q_{c1}, Q_{c2}	input oil volume flow rates of the vane chambers
C_{a1}, C_{a2}	hydraulic capacities of the vane chambers
V_{c1}, V_{c2}	oil volumes in the vane chambers
g_{c1}, g_{c2}	leak hydraulic conductances of the vane chambers
A_c	pressure-torque angular coefficient of the vane chambers
$x_p, \dot{x}_p$	pin position and pin velocity
m_p	mass of the pin
$b_p(\dot{x}_p)$	friction coefficient of the pin
$K_p(x_p)$	spring stiffness coefficient of the pin
A_p	area of the pin facing the first vane chamber
J_r, b_r	inertia and linear friction coefficients of the inner rotor
θ_r, θ_s	angular positions of inner and outer rotors
ω_r, ω_s	angular velocities of inner and outer rotors
θ_{rs}	relative angular position between the inner and outer rotors
ω_{rs}	relative angular velocity between the inner and outer rotors
$K_r(\omega_{rs})$	relative spring stiffness coefficient of inner and outer rotors
τ_r	external load torque acting on the inner rotor
τ_{rs}	spring torque between inner and outer rotors

TABLE I
MAIN PARAMETERS AND VARIABLES OF THE VVT SYSTEM.

1) The OCV valve: the actuator used for the phasing time control is a fast switching 4-way hydraulic valve modulated by Pulse-Width-Modulation (PWM) technique (see Fig. 5). The current I flowing into the solenoid generates a magnetomotive force which acts on the valve spring and moves the valve plunger. The plunger position completely defines the shape of the valve orifices and controls the oil pressure flows towards the vane chambers. By using the POG basic concepts and the energetic domain analogies described in [Zanasi, 1991] and [Zanasi, 2010], it can be shown that in steady-state conditions the dynamic model of the OCV valve becomes static and it can be described by a two dimensional nonlinear dissipative hydraulic resistance. The POG static model of the OCV valve is shown in Fig. 4 between the two power sections ① and ②. Vectors $\mathbf{P}_i$, $\mathbf{Q}_i$, $\mathbf{P}_d$, $\mathbf{Q}_d$, $\mathbf{Q}_{dc}$ and matrices $\mathbf{H}_1$, $\mathbf{H}_2$ are defined as follows:

$$\mathbf{P}_i = \begin{bmatrix} P \\ R \end{bmatrix}, \quad \mathbf{Q}_i = \begin{bmatrix} Q_p \\ Q_r \end{bmatrix}, \quad \mathbf{H}_1 = \begin{bmatrix} 1 & 0 \\ 1 & 0 \\ 0 & 1 \\ 0 & 1 \end{bmatrix}, \quad \mathbf{H}_2 = \begin{bmatrix} 1 & 0 \\ 0 & 1 \\ 1 & 0 \\ 0 & 1 \end{bmatrix},$$

$$\mathbf{P}_d = \begin{bmatrix} P - P_{c1} \\ P - P_{c2} \\ R - P_{c1} \\ R - P_{c2} \end{bmatrix} = \begin{bmatrix} P_{p1} \\ P_{p2} \\ P_{r1} \\ P_{r2} \end{bmatrix}, \quad \mathbf{Q}_d = \begin{bmatrix} Q_{p1}(P_{p1}, I) \\ Q_{p2}(P_{p2}, I) \\ Q_{r1}(P_{r1}, I) \\ Q_{r2}(P_{r2}, I) \end{bmatrix},$$

$$\mathbf{Q}_i = \mathbf{H}_1 \mathbf{Q}_d = \begin{bmatrix} Q_{p1} + Q_{p2} \\ Q_{r1} + Q_{r2} \end{bmatrix}, \quad \mathbf{Q}_{dc} = \mathbf{H}_2 \mathbf{Q}_d = \begin{bmatrix} Q_{p1} + Q_{r1} \\ Q_{p2} + Q_{r2} \end{bmatrix}.$$

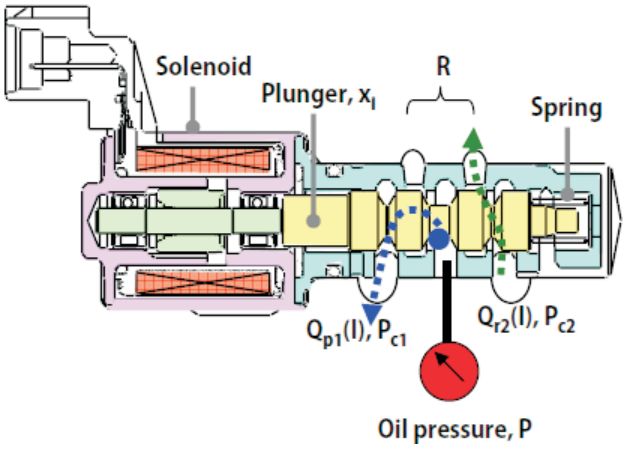

Fig. 5. The OCV valve. The oil volume flow rates, controlled by current I, flow through the orifices (in green and blue) and reach the vane chambers.

The oil volume flow rates Q_{p1}, Q_{p2}, Q_{r1}, Q_{r3} flowing from P and R towards the vanes chambers are defined as follows:

$$\begin{aligned} Q_{p1}(P_{p1}, I) &= C_{p1}(I)\sqrt{|P-P_{c1}|}\text{sign}(P-P_{c1}) \\ Q_{p2}(P_{p2}, I) &= C_{p2}(I)\sqrt{|P-P_{c2}|}\text{sign}(P-P_{c2}) \\ Q_{r1}(P_{r1}, I) &= C_{r1}(I)\sqrt{|R-P_{c1}|}\text{sign}(R-P_{c1}) \\ Q_{r2}(P_{r2}, I) &= C_{r2}(I)\sqrt{|R-P_{c2}|}\text{sign}(R-P_{c2}) \end{aligned} \tag{1}$$

In steady-state conditions the current I flowing in the valve solenoid completely determines the position x_i of the valve plunger, the shapes of the valve orifices and the values of the flow rates coefficients $C_{p1}(I)$, $C_{p2}(I)$, $C_{r1}(I)$ and $C_{r3}(I)$. These coefficients are usually provided by the constructor, but they can also be determined experimentally. Moreover, they can be easily simulated in Simulink by using simple look-up tables.

2) The pin: the dynamic model of the pin is shown in Fig. 4 between the two power sections ② and ③. A POG detailed model of the pin dynamics is shown in Fig. 6.

The dynamic model of the pin is described by the following differential and static equations:

$$\begin{aligned} m_p\ddot{x}_p &= \mathbf{A}_p\mathbf{P}_c - F_b - F_p \\ &= \begin{bmatrix} A_p & 0 \end{bmatrix}\begin{bmatrix} P_{c1} \\ P_{c2} \end{bmatrix} - b_p(\dot{x}_p)\dot{x}_p - F_p \\ &= A_p P_{c1} - b_p(\dot{x}_p)\dot{x}_p - F_p \end{aligned} \tag{2}$$

$$\mathbf{Q}_p = \mathbf{A}_p^{\mathrm{T}}\dot{x}_p = \begin{bmatrix} A_p \\ 0 \end{bmatrix}\dot{x}_p = \begin{bmatrix} A_p\dot{x}_p \\ 0 \end{bmatrix}$$

The pin moves subject to the forces generated by the vane chamber pressure P_{c1}, the viscous friction coefficient $b_p(\dot{x}_p)$ and the pin return spring $K_p(x_p)$. The nonlinear force $F_p = K_p(x_p)$ models both the force of the return spring and the contact force between the pin and the outer rotor case.

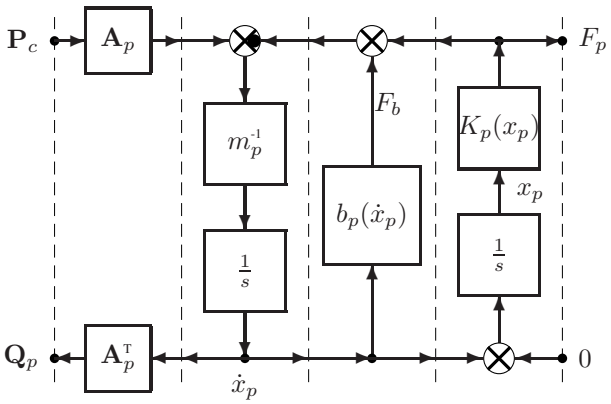

Fig. 6. POG detailed model of the pin dynamics.

3) The vane chambers: a detailed POG dynamic model of the vane chambers is shown in Fig. 4 between the two power sections ③ and ④. The pressures P_{c1} and P_{c2} of the vane chambers are determined by the oil volume flow rates $\mathbf{Q}_{dc}$, $\mathbf{Q}_r$, $\mathbf{Q}_r$ and $\mathbf{Q}_p$ entering the hydraulic capacities C_{a1} and C_{a2}: the flow rate $\mathbf{Q}_{dc}$ coming form the OCV valve through the orifices, the $\mathbf{Q}_r$ flow rate due to the inner rotor motion, $\mathbf{Q}_l$ flow rate due to the hydraulic losses of the vane chambers and the $\mathbf{Q}_p$ flow rates due to the pin motion. The very small capacity C_a stores potential energy in terms of oil pressure an it takes into account the high oil stiffness and the small elastic deformation of the valve case:

$$\begin{aligned} \mathbf{C}_a\dot{\mathbf{P}}_c &= \mathbf{Q}_{dc} - \mathbf{Q}_r - \mathbf{Q}_l - \mathbf{Q}_p \\ \mathbf{Q}_l &= \mathbf{G}_l(T_o)\mathbf{P}_c = \begin{bmatrix} g_{c1}(T_o)\,P_{c1} \\ g_{c2}(T_o)\,P_{c2} \end{bmatrix} \\ \mathbf{Q}_r &= \mathbf{A}_c^{\mathrm{T}}\omega_r = \begin{bmatrix} A_c \\ -A_c \end{bmatrix}\omega_r = \begin{bmatrix} A_c\omega_r \\ -A_c\omega_r \end{bmatrix}. \end{aligned} \tag{3}$$

The vectors $\mathbf{P}_c$, $\mathbf{Q}_c$, $\mathbf{A}_c^{\mathrm{T}}$ and the matrices $\mathbf{C}_a$, $\mathbf{G}_l$ shown in (3) and in the POG scheme of Fig. 4 are defined as follows:

$$\mathbf{P}_c = \begin{bmatrix} P_{c1} \\ P_{c2} \end{bmatrix}, \quad \mathbf{Q}_c = \begin{bmatrix} Q_{c1} \\ Q_{c2} \end{bmatrix}, \quad \mathbf{V}_c = \begin{bmatrix} V_{c1} \\ V_{c2} \end{bmatrix},$$

$$\mathbf{C}_a = \begin{bmatrix} C_{a1} & 0 \\ 0 & C_{a2} \end{bmatrix}, \quad \mathbf{G}_l = \begin{bmatrix} g_{c1} & 0 \\ 0 & g_{c2} \end{bmatrix}, \quad \mathbf{A}_c^{\mathrm{T}} = \begin{bmatrix} A_c \\ -A_c \end{bmatrix}.$$

The leak hydraulic coefficients g_{c1} and g_{c2} are usually function of the oil temperature T_o: $g_{c1} = g_{c1}(T_o)$ and $g_{c2} = g_{c2}(T_o)$.

4) The inner rotor: the POG dynamic model of the inner rotor is shown in Fig. 4 between the two power sections ④ and ⑤. Depending on the OCV plunger position the vane chambers can be connected to the power supply pressure P or to the return tank pressure R. The delta pressure $P_{c1}-P_{c2}$ between the chambers produces a torque τ_c acting

on the inner rotor. This torque acts against the cam bearing friction torque $\tau_r = f(\omega_r, To)$, the internal friction torque τ_b and the nonlinear internal spring torque $\tau_{rs} = K_r(\theta_{rs})$. The dynamic equations of the inner rotor with respect to the outer one are the following:

$$\begin{aligned} J_r\dot{\omega}_{rs} &= \mathbf{A}_c\mathbf{P}_c - \tau_b - \tau_r - \tau_{rs} \\ &= \begin{bmatrix} A_c & -A_c \end{bmatrix} \begin{bmatrix} P_{c1} \\ P_{c2} \end{bmatrix} - b_r(\omega_{rs})\omega_{rs} - \tau_r - \tau_{rs} \\ &= A_c(P_{c1} - P_{c2}) - b_r(\omega_{rs})\omega_{rs} - \tau_r - \tau_{rs} \\ \mathbf{Q}_r &= \mathbf{A}_c^{\mathrm{T}}\omega_{rs} = \begin{bmatrix} A_c \\ -A_c \end{bmatrix} \omega_{rs} = \begin{bmatrix} A_c\,\omega_{rs} \\ -A_c\,\omega_{rs} \end{bmatrix} \end{aligned} \tag{4}$$

The elastic torque τ_{rs} is also as function of pin state:

$$\tau_{rs} = \begin{cases} K_r(\omega_{rs}) & \text{when the } \textit{pin} \text{ is unlocked} \\ 0 & \text{when the } \textit{pin} \text{ is locked} \end{cases}$$

IV. Experimental set-up and model validation

The considered experimental set-up is shown in Fig. 8. The following electrical signals have been measured: cam position θ_r, oil temperature T_o, pump oil pressure P and engine angular speed ω_e. These signals have been used for model validation.

The engine angular speed ω_e has been measured using a magnetic pickup sensor, while the cam position θ_r has been measured using an Hall effect sensor. A post processing analysis was necessary to derive ω_e from the engine speed sensor and the cam phasing time from cam sensor. In this latter case a laborious work has been done for the TDC identification based on the signals pattern (see Fig. 9).

The results reported in Fig. 11, Fig. 12 and Fig. 13 have been normalized with respect to amplitude and time for reserve reasons. The good matching between the results obtained in simulation and the results obtained from the actual physical system are shown in Fig. 11. This good

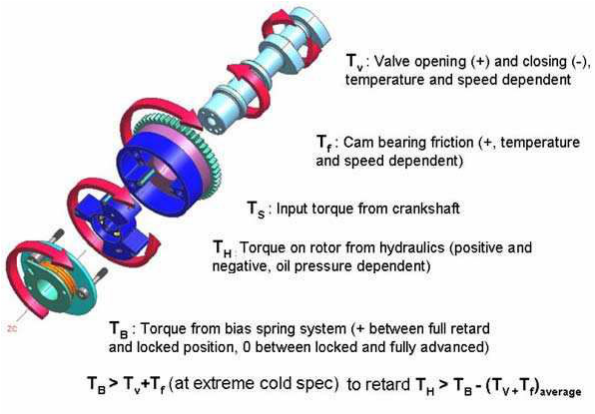

Fig. 7. Torque balancing in VVT system.

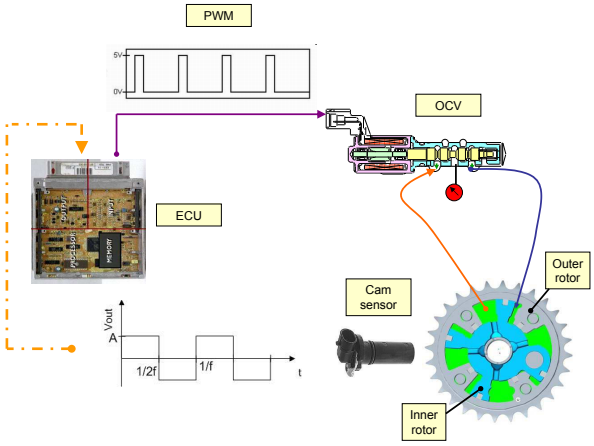

Fig. 8. Experimental set-up. By using the engine control unit inside the vehicle were spilled out the signals sensor needed for the model validation.

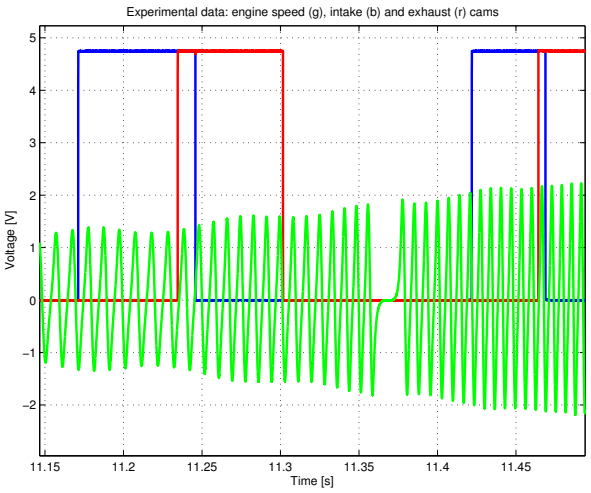

Fig. 9. Sensor signals captured.

matching confirms that the POG modeling technique based on an energetic approach is very useful for facing complex physical system. In particular, the obtained POG dynamic model is composed only by elementary blocks (integrator, summation elements, lookup tables, etc.) and therefore is useful when there are limited resources for the computational time of the embedded microcontroller.

The presented experimental results have been obtained as follows. Firstly the engine was warmed up until the oil temperature reached $90\,C^o$ and then the engine speed was increased up to around 2000 rpm: in this situation the VVT strategy was enabled and the cam phasing time was actuated. The cam phasing position has been controlled by using a simple discretized PID controller with a sampling time of 10 ms. Fig. 12 shows that when the VVT is off the control current is lower than the minimum actuation threshold, zero in this phase, and the chambers have a

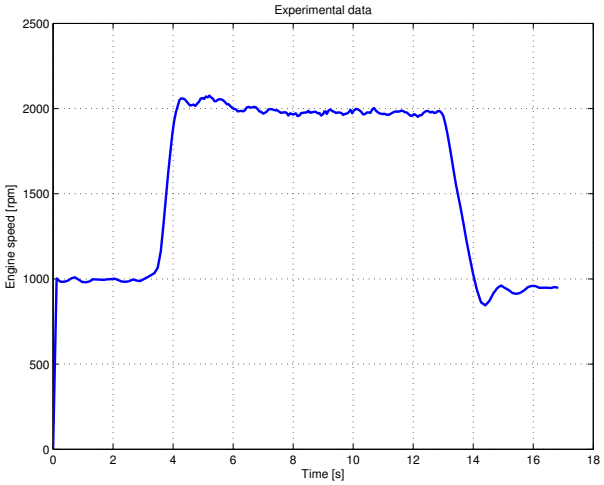

Fig. 10. Engine speed revolution.

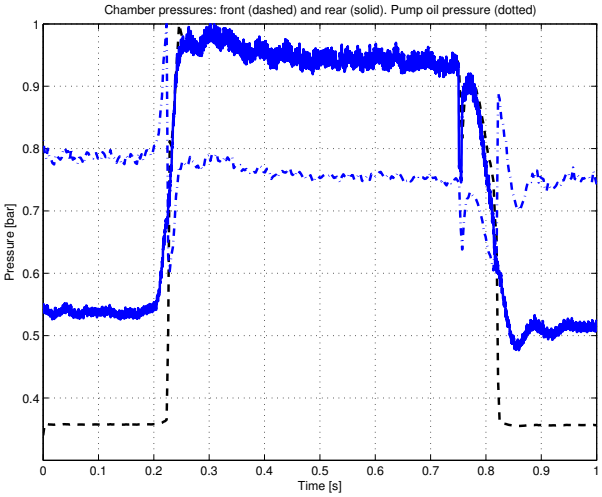

Fig. 12. Chambers and oil pressure normalized data.

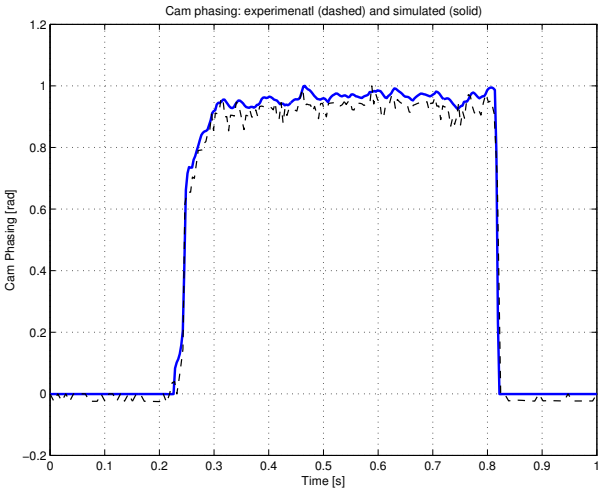

Fig. 11. Cam phasing: normalized comparison between simulation and experimental data.

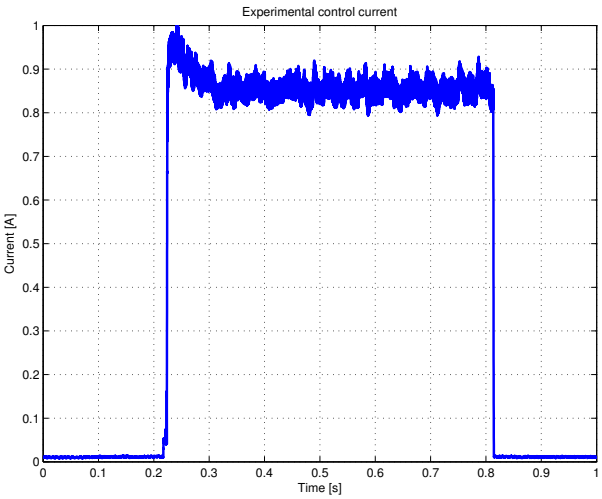

Fig. 13. Current control normalized data.

constant delta pressure because of the initial oil pressurized filling of the rear cam vane chamber (see Fig. 13).

When the duty cycle is applied, the control current increases (see Fig. 13), the OCV spool moves, the pressurized oil starts to flow in the advance chamber and the inner rotor starts to move with respect to the outer. Then, when the desired cam phasing position is reached, the two chambers reach a pressure which guarantees the balance between the motion and the resistance torque.

V. CONCLUSIONS

This paper proposes a control-oriented model of a variable valve timing (VVT) system on V12 Lamborghini engine. The POG modeling technique has been used to obtain a energy based model of the VVT. The simplicity of the POG modeling technique were able to well describe the main dynamic phenomena that affect the behavior of the system. Consequently the proposed model is a good starting point for studying the control strategy needed for improving the performance with regard to the engine emission without affecting the vehicle drivability. In future, the implementation on embedded target by code generation could be useful to validate the production code on the test rig. The POG technique represents a simple and fast way for modeling a multi domain physical system and can be applied also on the other engine subsystems.

REFERENCES

[Leone et al., 1999] Leone, T.G., E.J. Christenson and R.A. Stein (1996), *Comparison of variable camshaft timing strategies at part load"*, In: Proc. of the SAE Conference, number 960584.

[Gray, 1988] H. Bauer, *A review of variable engine valve timing"*, In: Proc. of the SAE Conference,number 880386.

[Ma, 1988] Ma, T. H, *Effects of variable engine valve timing on fuel economy"*, In: Proc. of the SAE Conference, number 880390.

[Stein and Galietti, 1995] Stein, R.A. and T.G. Galietti, K.M. an Leone *Dual equal VCT - a variable camshaft timing strategy for improved fuel economy and emissions*, In: Proc. of the SAE Conference, number 950975.

[Gauthier et al., 2005] Daniel G. Gauthier, Thomas H. Lichti and John H. Waller, *Improving cam phaser perfomrnace using robust engineering technique"*, SAE Technical Paper 2005-01-3903, 2005.

[Chauvin and Petit, 2007] Jonathan Chauvin, Nicolas Petit, *Nonlinear control of hydraulic camshaft actuators in variable cam timing enignes"*, In: Fifth IFAC Symposium on Advances in Automotive Control, United States, 2007

[Zanasi, 1991] R. Zanasi, *Power Oriented Modelling of Dynamical System for Simulation"*, IMACS Symp. on Modelling and Control of Technological System, Lille, France, May 1991.

[Zanasi, 2010] Zanasi, R. *The Power-Oriented Graphs technique: system modeling and basic properties*, IEEE VPPC 2010, Lille, France, September 2010

[Buchinger et al., 1998] Steinberg, R., Lenz, I., Koehnlein, G., Scheidt, M., Saupe, T and Buchinger, W., *A fully continuous variable valve timing concept for intake and exhaust phasing"*, SAE Technical Paper, number 98076.

[Stone et al., 1988] Stone, C.R. and Kwan, E., *Variable Valve Actuation mechanisms and the potential for their application"*, SAE Technical Paper, number 890673